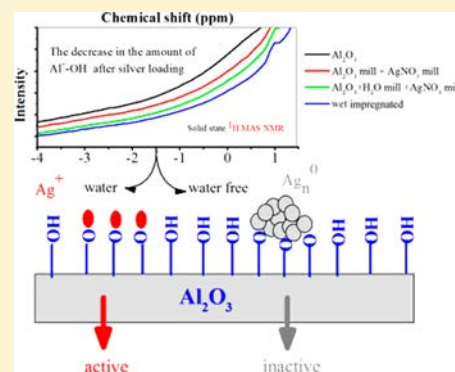


# Water Effect on Preparation of Ag/Al<sub>2</sub>O<sub>3</sub> Catalyst for Reduction of NO<sub>x</sub> by Ethanol

Hua Deng,<sup>†</sup> Yunbo Yu,<sup>†,‡</sup> and Hong He<sup>\*,†,‡</sup><sup>†</sup>Innovation Center for Excellence in Urban Atmospheric Environment, Institute of Urban Environment, Chinese Academy of Sciences, Xiamen 361021, China<sup>‡</sup>Research Center for Eco-Environmental Sciences, Chinese Academy of Sciences, Beijing, 100085, China

**ABSTRACT:** Alumina-supported silver catalysts (Ag/Al<sub>2</sub>O<sub>3</sub>) derived from wet impregnation, a semiwet method, and water-free ball-milling were investigated for the selective catalytic reduction of NO<sub>x</sub> by ethanol. It was found that Ag/Al<sub>2</sub>O<sub>3</sub> catalysts with the highest NO<sub>x</sub> reduction efficiency can be obtained via wet impregnation and the semiwet method but not by water-free ball milling. To optimize the preparation parameters and discern the effect of water in the production of Ag/Al<sub>2</sub>O<sub>3</sub> catalysts, the resulting series of alumina-supported silver samples were characterized by means of XRD, BET, XAS (XANES and EXAFS), in situ DRIFTS, and NMR. The results indicated that silver species were oxidized and highly dispersed on the large surface area Al<sub>2</sub>O<sub>3</sub> obtained from wet impregnation and the semiwet method. In situ DRIFTS revealed that the vital intermediate enolic species were correspondingly predominant on the surfaces of catalysts prepared by these methods, while the inactive intermediate acetate species were significantly formed on Ag/Al<sub>2</sub>O<sub>3</sub> catalysts prepared by water-free ball milling. Solid state <sup>1</sup>H NMR suggested that the water employed in the wet methods enhances the exchange of Ag<sup>+</sup> with protons from hydroxyl groups on the alumina surface, which leads to silver species being highly dispersed and forming active Ag–O–Al entities.



## 1. INTRODUCTION

Compared with lean-burn gasoline engines, the use of diesel engines has become a popular strategy to improve fuel economy. However, emission control, especially NO<sub>x</sub> abatement, is a major challenge for environmental catalysis under an oxidizing atmosphere.<sup>1–5</sup> Since the pioneering work of Iwamoto et al.<sup>6</sup> and Held et al.,<sup>7</sup> selective catalytic reduction of NO<sub>x</sub> by hydrocarbons (HC-SCR) has drawn more and more attention for the removal of NO<sub>x</sub> from lean-burn exhaust.<sup>8–10</sup> Among the available catalysts, Ag/Al<sub>2</sub>O<sub>3</sub> is deemed one of the most effective materials for HC-SCR of NO<sub>x</sub>.<sup>11,12</sup> In particular, when ethanol is used as a reductant, good activity<sup>13,14</sup> and moderate tolerance to water and SO<sub>2</sub> can be achieved.<sup>15</sup> Currently, the low-temperature activity<sup>16,17</sup> (<350 °C) of Ag/Al<sub>2</sub>O<sub>3</sub> and the complexity of its preparation still remain bottlenecks for the development of HC-SCR.

Understanding the structure of Ag/Al<sub>2</sub>O<sub>3</sub> catalysts at the molecular or atomic level opens a window to enable solution of these problems. Numerous studies have shown that both the support and silver loading are critical in producing an active Ag/Al<sub>2</sub>O<sub>3</sub> catalyst. Over this catalyst, oxidized silver (Ag<sup>+</sup> and/or Ag<sub>n</sub><sup>δ+</sup>) rather than metallic silver species are believed to be the active species for catalysis of the reduction of NO<sub>x</sub> by hydrocarbons.<sup>18–20</sup> Moreover, entities at the interface of the metal and support like Ag–O–Al were found to be highly active in the reduction of NO<sub>x</sub> by methane.<sup>21</sup> In surface mechanism studies, Burch et al.<sup>22</sup> and Yu et al.<sup>23</sup> found that the

interface between active silver and alumina plays a very important role in activating vital intermediate isocyanate species (–NCO) and enolic species (RCH = CH–O<sup>–</sup>) respectively. Recently, On the basis of solid-state nuclear magnetic resonance (NMR) results and density functional theory (DFT) simulation of the structure of Ag–O–Al entities, we found that oxidized Ag<sup>+</sup> anchored on the Al tetrahedral site of alumina, forming the Ag–O–Al<sub>tetra</sub> entity, is vital to the excellent catalytic performance of Ag/Al<sub>2</sub>O<sub>3</sub>.<sup>24,25</sup>

To design a highly efficient Ag/Al<sub>2</sub>O<sub>3</sub> catalyst for application in HC-SCR systems, many preparation methods have been tested. Wet impregnation,<sup>18,20,23–26</sup> coprecipitation,<sup>21,27</sup> sol-gel processes,<sup>26,28,29</sup> and solvent-free ball-milling treatments<sup>17</sup> have been reported. In general, wet impregnation from aqueous solution with AgNO<sub>3</sub> as a precursor has been able to produce the highest activity Ag/Al<sub>2</sub>O<sub>3</sub> catalysts.<sup>17,26</sup> However, the role of the solution or water in the preparation of the catalyst still remains an open question.

In this study, the NO<sub>x</sub> removal efficiency of Ag/Al<sub>2</sub>O<sub>3</sub> catalysts derived from the wet impregnation method, semiwet method, and water-free ball-milling method was compared. The effect of water in preparation of the catalyst was addressed by analyzing a variety of characterization results. It was found that

Received: September 2, 2016

Revised: September 29, 2016

Published: September 29, 2016

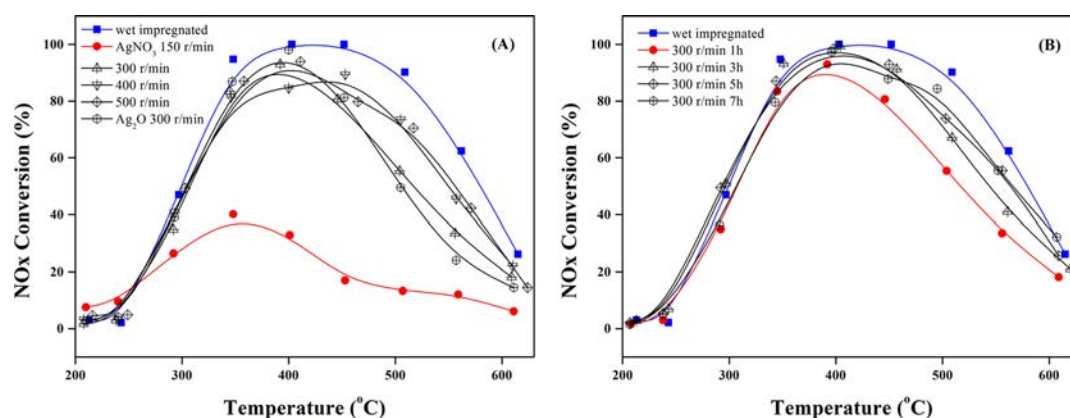


**Figure 1.** NO<sub>x</sub> conversion for SCR by C<sub>2</sub>H<sub>5</sub>OH over Ag/Al<sub>2</sub>O<sub>3</sub> catalysts prepared by dry ball-milling method: (A) rotation speed and (B) rotation time.

water is vital for forming highly dispersed active Ag–O–Al entities. Solid-state <sup>1</sup>H NMR results indicated that water enhances the exchange of silver with surface hydroxyl groups (Al<sup>3+</sup>–OH) via a proton exchange mechanism.

## 2. MATERIALS AND METHODS

**2.1. Materials Preparation. Water-Free Ball-Milling Method.** Ag/Al<sub>2</sub>O<sub>3</sub> catalysts (2 wt %) were prepared by water-free ball-milling (dry method) using AgNO<sub>3</sub> or Ag<sub>2</sub>O as the silver precursor. Typically, an appropriate amount of silver precursor and 25 g of γ-Al<sub>2</sub>O<sub>3</sub> (SASOL, SBa-200) were mixed in a 500 cm<sup>3</sup> sintered alumina oxide grinding jar with several 10 and 5 mm diameter sintered alumina grinding balls. The milling procedure was performed in a Retsch PM100 Planetary ball mill at different rotation speeds (150, 300, 400, and 500 r/min, respectively). At fixed rotation speed, the effects of different rotation times (1, 3, 5, and 7 h, respectively) were also compared. The resulting powders were calcined at 600 °C for 3 h.

**Wet Impregnated Method.** Catalysts were also prepared by wet impregnation (wet method) as a comparison.<sup>24,25</sup> An appropriate amount of γ-Al<sub>2</sub>O<sub>3</sub> (SASOL, SBa-200) was immersed in an aqueous solution of silver nitrate to obtain 2 wt % silver loading. After stirring for 1 h, the excess water was removed by a rotary evaporator under vacuum at 60 °C. Then, the samples were calcined in a furnace at 600 °C for 3 h.

**Semi Wet Method.** On the basis of these dry and wet catalyst preparation methods, a new semiwet method was explored. A fixed amount of water (solid–liquid ratio = 5, 2.5, and 1.25 g/mL, respectively) was added to Al<sub>2</sub>O<sub>3</sub> or a mixture of AgNO<sub>3</sub> and Al<sub>2</sub>O<sub>3</sub> before the ball-milling process (300 r/min, 1 h). The resulting silver-loaded powders were also calcined at 600 °C for 3 h. The Ag content of the catalysts was determined by ICP-OES to be ~2 wt %. Before activity testing, the catalysts were crushed and sieved to a diameter range from 0.25 to 0.42 mm.

**2.2. Catalytic Measurements.** A gaseous mixture of NO (800 ppm), C<sub>2</sub>H<sub>5</sub>OH (1565 ppm), water vapor (10%), and O<sub>2</sub> (10%) in N<sub>2</sub> balance at a mass flow of 1 L min<sup>-1</sup> was accurately fed into the experimental reactor filled with 0.3 g catalysts, as described in our previous studies.<sup>23–25,27</sup> The concentrations of NO, NO<sub>2</sub>, N<sub>2</sub>O, NH<sub>3</sub>, and CO were analyzed online simultaneously by an FTIR spectrometer (Nicolet Nexus iS10). The details of the experimental setup can be found in our previous work.<sup>23–25</sup> In all of the experiments, the

concentration of N<sub>2</sub>O was negligible, and thus NO<sub>x</sub> conversion can be calculated using the following equation

$$\text{NO}_x \text{ conversion (\%)} = \frac{[\text{NO}]_{\text{in}} + [\text{NO}_2]_{\text{in}} - [\text{NO}]_{\text{out}} - [\text{NO}_2]_{\text{out}}}{[\text{NO}]_{\text{in}} + [\text{NO}_2]_{\text{in}}} \times 100\%$$

The N<sub>2</sub> selectivity was defined as follows

$$\text{N}_2 \text{ selectivity (\%)} = \frac{[\text{NO}]_{\text{in}} + [\text{NO}_2]_{\text{in}} - [\text{NO}]_{\text{out}} - [\text{NO}_2]_{\text{out}} - [\text{NH}_3]_{\text{out}}}{[\text{NO}]_{\text{in}} + [\text{NO}_2]_{\text{in}}} \times 100\%$$

**2.3. Catalyst Characterization.** The X-ray powder diffraction patterns of the various catalysts were collected on a Rigaku D/max-RB X-ray diffractometer (Japan). The patterns were run with Cu Kα radiation (λ = 1.5406 Å) at 40 kV and 40 mA with a scanning speed of 5°/min. The patterns were taken over the 2θ range from 10 to 90°.

Nitrogen adsorption–desorption isotherms were measured using a Quantachrome Autosorb-1C instrument at 77 K. The specific surface area of the samples was calculated by the Brunauer–Emmett–Teller (BET) method. The pore volume and size distribution were determined by the Barrett–Joyner–Halenda (BJH) method from the desorption branches of the isotherms.

The XANES and EXAFS of Ag–K edges were measured in transmission mode at room temperature on the BL14W1 beamline, Shanghai Synchrotron Radiation Facility (SSRF), Shanghai China. Ag foil and AgNO<sub>3</sub> were used as references. The storage ring was operated at 6.5 GeV with 50 mA as an average storage current. The synchrotron radiation beamline was monochromatized with a Si (3 1 1) double-crystal monochromator, and mirrors were used to eliminate higher harmonics. Before measurements, all samples were crushed and sieved to 200 mesh or finer and then diluted with flour powder at appropriate ratios and pressed into thin disks.

XANES and XAFS data were analyzed by the Demeter 9 software package.<sup>30</sup> XANES spectra were normalized with edge height; then, the first-order derivatives were taken to compare the variation of absorption edge energies. EXAFS oscillation χ(k) was extracted using spline smoothing and weighted by k<sup>3</sup> to compensate for the diminishing amplitude in the high k range. The filtered k<sup>3</sup>-weighted χ(k) was transformed to R space in the k range of 2 to 9 Å<sup>-1</sup> with a Hanning function window.

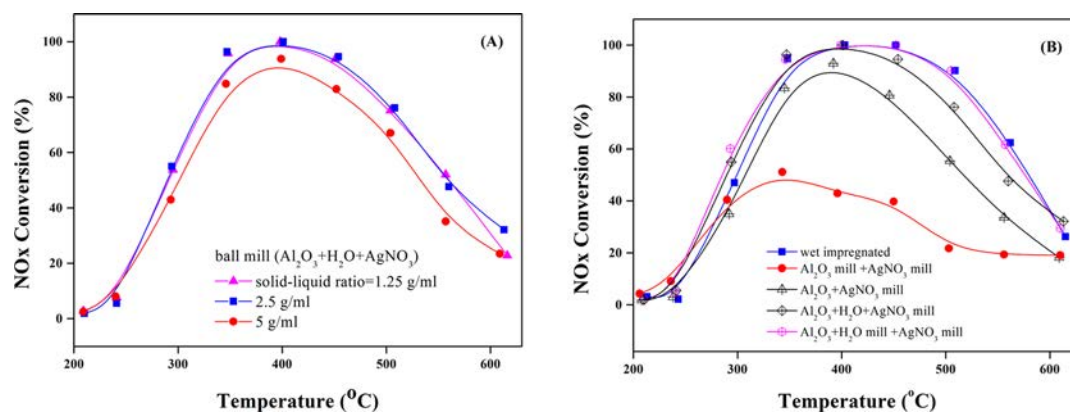


**Figure 2.** NO<sub>x</sub> conversion for SCR by C<sub>2</sub>H<sub>5</sub>OH over Ag/Al<sub>2</sub>O<sub>3</sub> catalysts prepared by wet ball-milling method: effect of (A) water amount and (B) rotation process.

In situ diffuse reflectance infrared Fourier transform spectroscopy (DRIFTS) spectra were recorded on a Nexus 670 FT-IR (Thermo Nicolet), equipped with an in situ diffuse reflection chamber and a high-sensitivity MCT/A detector. All Ag/Al<sub>2</sub>O<sub>3</sub> catalysts were finely ground and placed in ceramic crucibles in the in situ chamber. Prior to recording each DRIFTS spectrum, the sample was heated in situ in 10% O<sub>2</sub>/N<sub>2</sub> flow at 823 K for 1 h, then cooled to the desired temperature to measure a reference spectrum. All spectra were measured with a resolution of 4 cm<sup>-1</sup> and with an accumulation of 100 scans.

All <sup>1</sup>H MAS NMR experiments were performed at room temperature (303 K) on a Bruker 400 MHz WB solid-state NMR spectrometer, operating at a magnetic field of 9.4 T. The spectrometer frequency is 400.25 for <sup>1</sup>H. All of the spectra were acquired at a sample spinning rate of 6.5 kHz with a 7 mm ZrO<sub>2</sub> MAS rotor. A 90° single pulse of 4.5 μs was used. Each spectrum was acquired using a total of 64 scans with a recycle delay time of 4 s and an acquisition time of 0.013 s. All spectra were externally referenced (i.e., the 0 ppm position) to sat. aqueous DSS. The raw spectral data were normalized by weight, where constant or known weights of samples were recorded.

### 3. RESULTS AND DISCUSSION

**3.1. Catalytic Activity of Ag/Al<sub>2</sub>O<sub>3</sub>.** To examine the effect of ball-mill rotation parameters on the activity of Ag/Al<sub>2</sub>O<sub>3</sub> catalysts in the reduction of NOx by ethanol, different rotation speeds ranging from 150 to 500 r/min for 1 h were used to prepare the catalysts. At a fixed rotation speed of 300 r/min, increasing the rotation time (3, 5, and 7 h) was also considered. Figure 1 compares the NOx conversion as a function of temperature over catalysts obtained by the ball-milling and wet impregnation methods. The effect of rotation speed was significant, as shown in Figure 1A. At the lowest rotation speed of 150 r/min and AgNO<sub>3</sub> as silver precursor, a maximum NOx conversion of 40% was obtained at 348 °C. Increasing the rotation speed to 300 and 500 r/min significantly enhanced the NOx conversion. For instance, at the rotation speed of 300 r/min, NOx conversion of 93% could be achieved at 392 °C. However, surpassing this rotation speed did not enhance the NOx conversion except for the slight promotion of catalytic activity in the high-temperature region (above 400 °C). Therefore, the rotation operating conditions were 300 r/min for 1 h in subsequent experiments.

As a comparison, silver oxide (Ag<sub>2</sub>O) also was used as silver precursor to prepare Ag/Al<sub>2</sub>O<sub>3</sub> by the ball-milling method at 300 r/min, and similar activity was found to that prepared from the AgNO<sub>3</sub> precursor. The wet impregnation method, which has always been considered as the best way to prepare Ag/Al<sub>2</sub>O<sub>3</sub> catalysts,<sup>17,26</sup> was also tested in this study. It was confirmed that wet impregnation produced the best catalysts among all samples in the reduction of NOx. As shown in Figure 1B, increasing the rotation time from 1 to 7 h at a fixed speed of 300 r/min was helpful in improving the activity. However, these ball-milled samples were still worse than the wet impregnated sample.

The major difference between the dry method of ball-milling and the wet impregnation method was the absence of water. Because the wet-impregnated sample was the best catalyst among all samples prepared, a semiwet ball-milling method was explored. A trace amount of water was added to the mixture of Al<sub>2</sub>O<sub>3</sub> and AgNO<sub>3</sub> during the dry ball-milling. The effect of the water amount is examined in Figure 2A in terms of NOx conversion. It can be clearly seen that the optimum water amount (ratio of solid to liquid) was ~2.5 g/mL. On increasing the ratio to 1.25 g/mL, the NOx conversion was almost unchanged. If the amount of water kept increasing, then the dry ball-milling method would fail and would simply become the wet impregnation method. However, on decreasing the water amount to a ratio of 5 g/mL, the NOx conversion was significantly depressed.

To understand the water effect, we explored different semiwet ball-milling processes, as shown in Figure 2B. Ball-milling the bare Al<sub>2</sub>O<sub>3</sub> at 300 r/min for 1 h prior to adding and grinding the AgNO<sub>3</sub> precursor in the mixture resulted in a significant decrease in NOx conversion. However, ball-milling the mixture of silver and alumina together with water boosted the catalytic activity significantly, and this catalyst was more active than the sample prepared without water. Ball-milling the bare Al<sub>2</sub>O<sub>3</sub> together with water prior to adding AgNO<sub>3</sub> and then further milling the mixture lead to the maximum NOx reduction activity. The catalyst resulting from this preparation method not only exhibited the same activity as the best wet-impregnated sample but also avoided complicated steps necessary in the wet method process, such as vaporization of excess water. In summary, the semiwet method shows considerable potential as a substitute for the traditional wet impregnation process for preparing Ag/Al<sub>2</sub>O<sub>3</sub> catalysts.

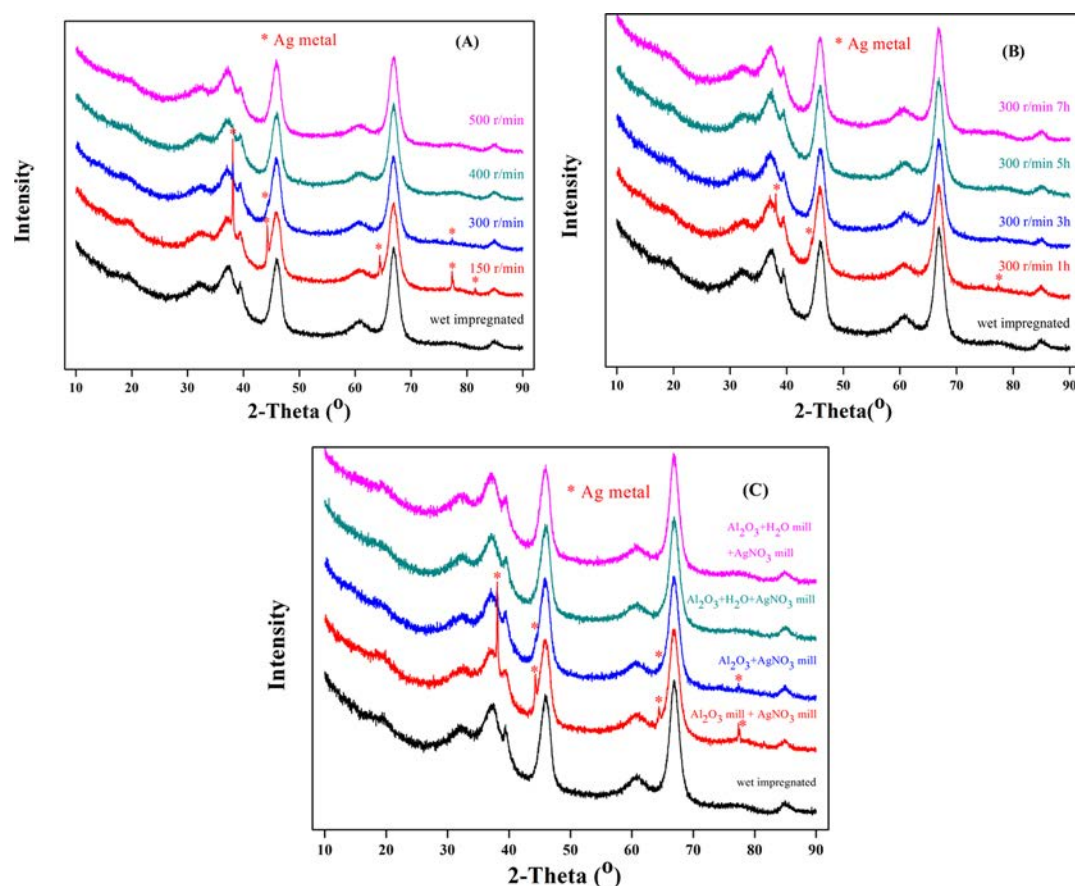


**Figure 3.** XRD patterns of 2 wt % Ag/Al<sub>2</sub>O<sub>3</sub> catalysts prepared by different methods: (A) rotation speed, (B) rotation time, and (C) rotation process.

**3.2. Catalyst Characterization.** XRD patterns of all Ag/Al<sub>2</sub>O<sub>3</sub> catalysts are exhibited in Figure 3.  $\gamma$ -Al<sub>2</sub>O<sub>3</sub> (JCPDS reference no. 00-010-0425) was the main phase detected for all samples with silver loading of 2 wt %, indicating that the silver species are highly dispersed. In our previous study,<sup>31</sup> XRD peaks for the metallic Ag and Ag<sub>2</sub>O phases were observed only for high silver loading of 8 wt %. However, the sample with silver loading of 2 wt % prepared by ball-milling at the low rotation speed of 150 r/min (Figure 3A) also exhibited peaks for the Ag metallic phase, indicating the aggregation of silver species. A similar result was found for the sample prepared by ball-milling bare Al<sub>2</sub>O<sub>3</sub> prior to adding silver precursors (as shown in Figure 3 C). The appearance of peaks attributable to silver metal along with poor activity suggests that highly dispersed silver species, especially oxidized species,<sup>18–21,23–25</sup> might be the active sites. Because the dry method was employed without the use of water, the silver precursor crystals might not be dispersed efficiently at low rotation speed. On addition of water in the semiwet preparation method, no peaks indexed to silver metal could be found (as shown in Figure 3 C). Thus, a conclusion can be drawn that a trace amount of water is beneficial for the dispersion of silver species. The BET surface areas of various catalysts are also summarized in Table 1 to examine the differences in physical structure.

The results show that the specific surface areas were in the range from 158 to 197 m<sup>2</sup> g<sup>-1</sup> for all Ag/Al<sub>2</sub>O<sub>3</sub> catalysts. Increasing the rotation speed and time resulted in a gradual decrease in the surface area and pore volume, while the pore diameter remained unchanged. It should be noted that the

**Table 1.** Textural Parameters of Ag/Al<sub>2</sub>O<sub>3</sub> Catalysts Prepared by Different Methods Derived from N<sub>2</sub> Physorption Results

sample	BET (m <sup>2</sup> /g)	pore volume (mL/g)	mean pore diameter (nm)
Al <sub>2</sub> O <sub>3</sub>	186	0.491	10.5
wet-impregnated	198	0.516	10.5
150 r/min	187	0.478	10.2
300 r/min	176	0.442	9.89
400 r/min	171	0.431	10.1
500 r/min	158	0.388	9.98
300 r/min 3h	174	0.427	9.96
300 r/min 5h	167	0.414	9.88
300 r/min 7h	163	0.392	9.49
(mill condition: 300 r/min 1 h)			
Al <sub>2</sub> O <sub>3</sub> mill + AgNO <sub>3</sub> mill	167	0.453	10.7
Al <sub>2</sub> O <sub>3</sub> + H <sub>2</sub> O mill + AgNO <sub>3</sub> mill	179	0.432	9.67
Al <sub>2</sub> O <sub>3</sub> + H <sub>2</sub> O + AgNO <sub>3</sub> mill	189	0.429	9.21

surface area followed the order: wet impregnation > semiwet method > water-free ball-milling. The catalysts prepared in the presence of water exhibited higher surface area than those without water, indicating that water is favorable to maintaining the basic physical structure of Al<sub>2</sub>O<sub>3</sub>.

To determine the precise chemical state of the supported silver, we compared the Ag–K XANES of Ag/Al<sub>2</sub>O<sub>3</sub> samples prepared by different methods with spectra of AgNO<sub>3</sub> and Ag foil, as shown in Figure 4. It can be clearly seen in Figure 4A

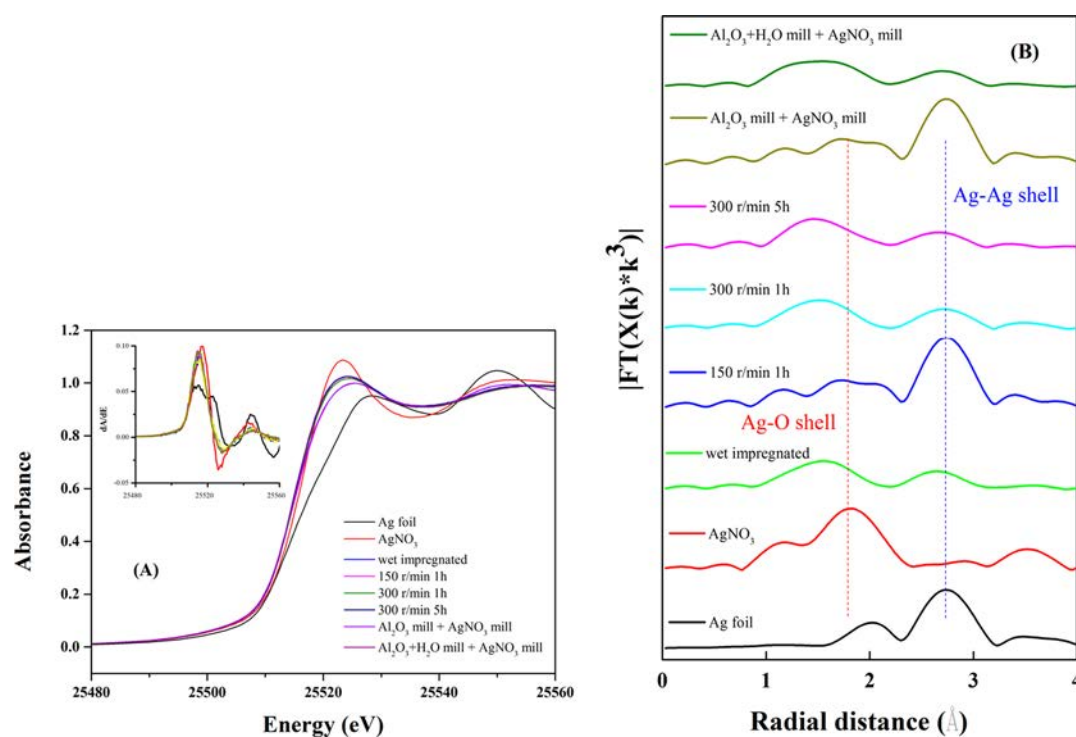


**Figure 4.** Normalized Ag–K XANES and first-order derivatives (A) and EXAFS spectra of Ag/Al<sub>2</sub>O<sub>3</sub> catalysts prepared by different methods, AgNO<sub>3</sub>, and Ag foil (B).

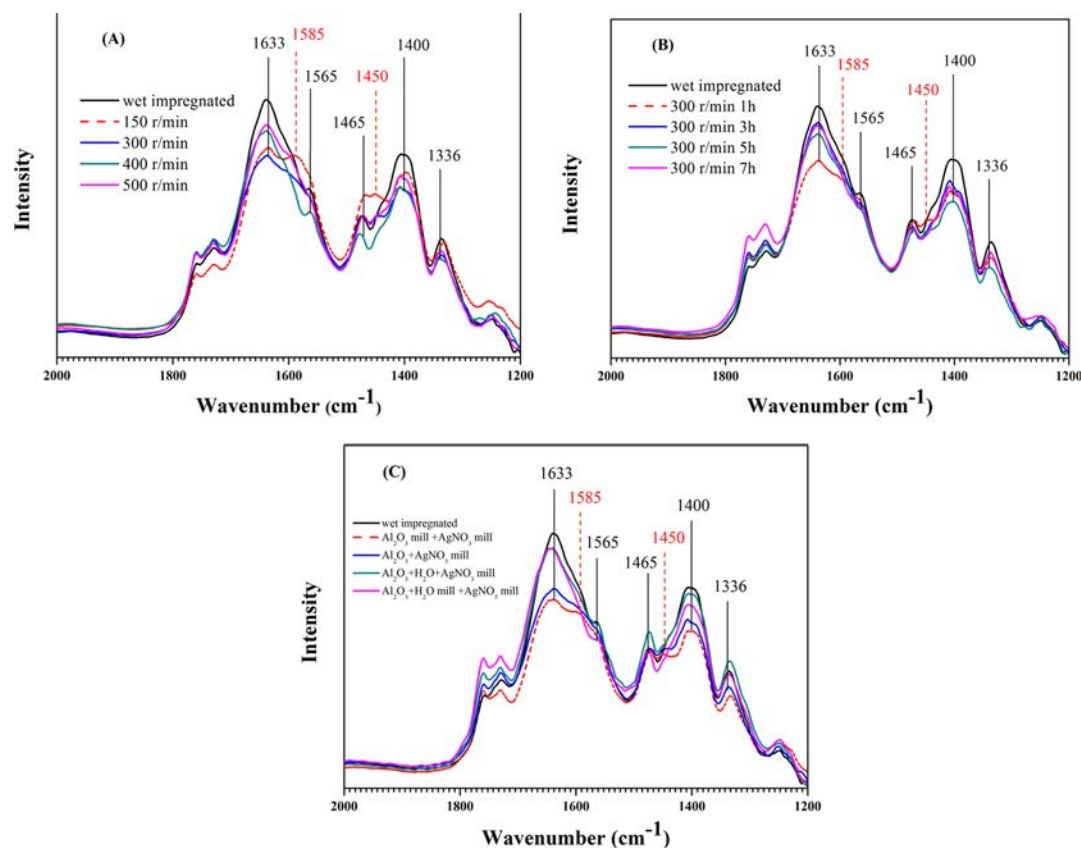


**Figure 5.** In situ DRIFTS spectra of adsorbed species on 2 wt % Ag/Al<sub>2</sub>O<sub>3</sub> catalysts prepared by different methods at steady state in a flow of C<sub>2</sub>H<sub>5</sub>OH+O<sub>2</sub>, as a function of (A) rotation speed, (B) rotation time, and (C) rotation process.

that the Ag/ $\gamma$ -Al<sub>2</sub>O<sub>3</sub> catalysts and AgNO<sub>3</sub> show similar Ag–K absorption edge energies, which are lower than that of Ag foil.

It has been reported that Ag has lower binding energy with increasing oxidation state due to its core-level photo-

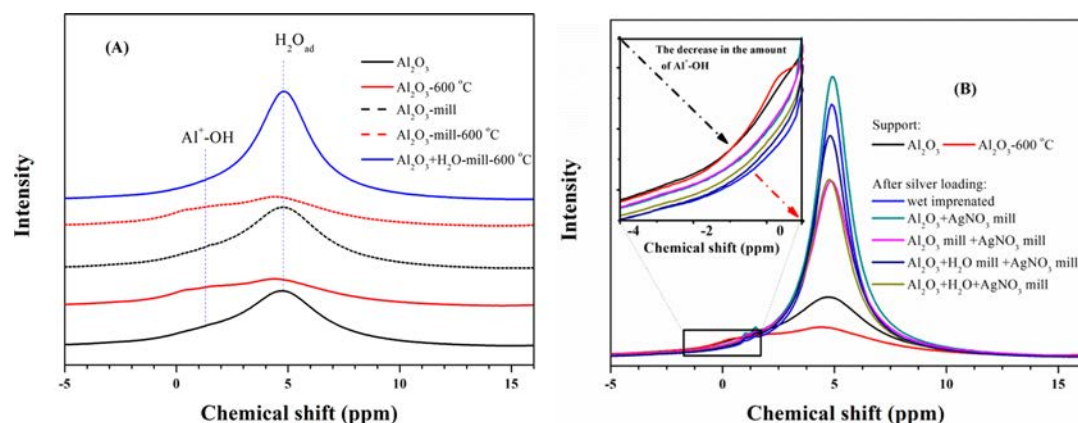


**Figure 6.** Solid-state  $^1\text{H}$  MAS NMR spectra of  $\text{Al}_2\text{O}_3$  and 2 wt %  $\text{Ag}/\text{Al}_2\text{O}_3$  catalysts (A)  $\text{Al}_2\text{O}_3$  and (B)  $\text{Ag}/\text{Al}_2\text{O}_3$ .

emission.<sup>18,28</sup> According to this empirical rule, supported silver species for all samples are mostly close to the +1 oxidation state, just like  $\text{Ag}^+$  ion in  $\text{AgNO}_3$  solid, even though silver metal XRD peaks were found for “150 r/min” and “ $\text{Al}_2\text{O}_3$  mill +  $\text{AgNO}_3$  mill” samples.

Figure 4B shows the Fourier transforms of  $k^3$ -weighted EXAFS oscillations at the Ag K-edge. A bond distance in the range of 1.75 to 2.5 Å was observed over all  $\text{Ag}/\text{Al}_2\text{O}_3$  samples, which can be assigned to an Ag–O shell. A peak at ca. 2.7 Å could be due to backscattering from adjacent silver atoms.<sup>26,32,33</sup> For all  $\text{Ag}/\text{Al}_2\text{O}_3$  samples (impregnated, 300 r/min 1 h, 300 r/min 5 h,  $\text{Al}_2\text{O}_3 + \text{H}_2\text{O}$  mill +  $\text{AgNO}_3$  mill), the peak of the Ag–O shell is predominant, suggesting that silver species are highly dispersed in the oxidized state, which play a very important role in the HC-SCR process.<sup>18–21,23–26,33</sup> An Ag–Ag shell is clearly predominant in the samples “150 r/min” and “ $\text{Al}_2\text{O}_3$  mill +  $\text{AgNO}_3$  mill”. This indicates that the active component silver species are not effectively dispersed but rather aggregate together, which is detrimental to catalysis of the reduction of  $\text{NO}_x$  by ethanol, as shown in Figures 1 and 2. Therefore, we can conclude that the preparation method is crucial for  $\text{Ag}/\text{Al}_2\text{O}_3$  catalysts. High dry-milling speed and long rotation time are both helpful to increase the dispersion of silver species. Meanwhile, the addition of water can easily optimize the interaction between silver species and the support  $\text{Al}_2\text{O}_3$ . However, the mechanism of how water enhances the dispersion of active silver species has not been revealed in depth.

**3.3. In Situ DRIFTS Study.** It is well known that the key to the HC-SCR of  $\text{NO}_x$  over  $\text{Ag}/\text{Al}_2\text{O}_3$  catalysts lies in the surface mechanism. HC-SCR of  $\text{NO}_x$  usually starts with the partial oxidation of the reductant, and thus in situ DRIFTS spectra were collected over different  $\text{Ag}/\text{Al}_2\text{O}_3$  samples in a flow of  $\text{C}_2\text{H}_5\text{OH}$  (1565 ppm) +  $\text{O}_2$  (10%) over the temperature range 200–500 °C. For convenience of comparison, Figure 5 shows the in situ DRIFT spectra at the reaction temperature of 300 °C over different  $\text{Ag}/\text{Al}_2\text{O}_3$  catalysts.

Exposure of different samples to the feed gas resulted in the appearance of seven peaks (1633, 1585, 1565, 1465, 1450, 1400, 1336  $\text{cm}^{-1}$ ) within the range of 2000–1200  $\text{cm}^{-1}$ . According to our previous studies,<sup>31,34,35</sup> peaks at 1633 and 1410 together with 1336  $\text{cm}^{-1}$  were assigned to the asymmetric and symmetric stretching vibrations and C–H deformation vibration of adsorbed enolic species, respectively. Peaks at 1585, 1565, 1465, and 1450  $\text{cm}^{-1}$  were due to acetate species adsorbed on the catalyst surface.<sup>26,36</sup> The partially oxidized

species, especially the enolic species, were identified as important intermediates in the ethanol-SCR process because of their higher activity toward  $\text{NO} + \text{O}_2$  than acetate, even though the latter was also formed during the partial oxidation of ethanol.<sup>15,18,23,25,31,34,35</sup>

It can be clearly seen in Figure 5 that the samples showing the characteristic XRD pattern peaks of metallic silver were covered by both enolic and acetate species equally. For instance, the dry ball-milling sample prepared at 150 r/min exhibited strong peaks of both enolic and acetate species, while samples with well-dispersed silver species, such as wet-impregnated  $\text{Ag}/\text{Al}_2\text{O}_3$ , were dominated by enolic species. Increasing the rotation time or adding water to the mixture made the enolic species' absorbance peak sharp, indicating that well-dispersed silver species are favorable to the formation of active partially oxidized intermediates. This was consistent with other reports<sup>19,25</sup> that metallic silver resulted in complete combustion of ethanol. Thus minimizing the concentration of large silver particles was necessary to improve the efficiency of  $\text{NO}_x$  reduction. Compared with improving mechanical factors like rotation speed, adding a trace amount of water was more facile and effective.

**3.4. Effect of Water on Dispersion of Silver Species.**  $\gamma$ - $\text{Al}_2\text{O}_3$  is one of the most commonly used supports for heterogeneous catalysts. A defect spinel lattice structure is terminated by surface hydroxyl groups,<sup>37</sup> which play an important role in determining the surface chemistry of the resulting catalysts. During the preparation of  $\text{Ag}/\text{Al}_2\text{O}_3$  catalysts, the silver species might interact with the alumina hydroxyl groups to produce dispersed silver oxide phases. To determine the effect of water on the preparation of catalysts, we compare the  $^1\text{H}$  MAS NMR spectra of  $\gamma$ - $\text{Al}_2\text{O}_3$  and  $\text{Ag}/\text{Al}_2\text{O}_3$  in Figure 6.

Resonances centered at 5 ppm that have been assigned to hydroxyl groups produced when water is adsorbed on to alumina<sup>38,39</sup> can be clearly seen in Figure 6A, while the shoulder resonance at 1 ppm can be attributed to the basic and acidic hydroxyl groups of alumina.<sup>38,39</sup> Calcination of  $\text{Al}_2\text{O}_3$  (as shown in Figure 6A) in air at 600 °C resulted in a decrease in the observed resonance at 5 ppm, but the addition of water caused a considerable increase in the intensity of the resonance at 5 ppm. The corresponding changes were expected because we have attributed them to hydroxyl groups produced when water is adsorbed. It should be noted that calcination of  $\text{Al}_2\text{O}_3$  did not cause considerable changes in the resonance centered at 1 ppm. Moreover, the resonance intensity of hydroxyl groups in

the range from  $-5$  to  $15$  ppm was almost unchanged whether the  $\text{Al}_2\text{O}_3$  support was ball-milled or not.

Because the sample was exposed to the ambient atmosphere, a resonance to physisorbed water on spectra can be easily found, which is consistent with other literature.<sup>39</sup> It is commonly accepted that the acidic hydroxyl groups and especially the basic OH groups are the anchoring sites for metal species.<sup>38</sup> After silver loading, the  $^1\text{H}$  MAS NMR spectra of  $\text{Ag}/\text{Al}_2\text{O}_3$  derived from different preparation methods were compared with those of the support  $\text{Al}_2\text{O}_3$ , as shown in Figure 6B. The intensity order of resonances attributed to basic and acidic OH groups on different samples was as follows:  $\text{Al}_2\text{O}_3 \approx \text{Al}_2\text{O}_3\text{-}600^\circ\text{C} > \text{Al}_2\text{O}_3 \text{ mill, then } + \text{AgNO}_3 \text{ mill} \approx \text{Al}_2\text{O}_3 + \text{AgNO}_3, \text{ mill} > \text{Al}_2\text{O}_3 + \text{H}_2\text{O} + \text{AgNO}_3, \text{ mill} > \text{Al}_2\text{O}_3 + \text{H}_2\text{O} \text{ mill, then } + \text{AgNO}_3 \text{ mill} > \text{wet impregnation}$ . It is suggested that silver species can exchange with protons from both acidic and basic OH groups on alumina. Water addition enhanced the degree of proton exchange, which is favorable to the formation of well-dispersed silver species. On the basis of this result, we can hypothesize that selecting a more suitable solvent may enable the preparation of advanced  $\text{Ag}/\text{Al}_2\text{O}_3$  catalysts.

#### 4. CONCLUSIONS

For the ethanol-SCR process, it was found that the general order of  $\text{NO}_x$  reduction efficiency as affected by preparation method can be described as wet impregnation  $\approx$  semiwet method  $\gg$  water-free ball milling. Among them, the semiwet method not only produced the highest activity catalyst but also can be implemented conveniently. Metallic silver species can be found on catalysts prepared by the water-free ball milling method, which indicates that silver species are not dispersed effectively. As a consequence, predominantly inactive intermediates like acetate species are formed on their surfaces, which lower the efficiency of  $\text{NO}_x$  removal. On the contrary, water in catalyst preparation plays a very important role in maintaining silver species in a highly dispersed and oxidized state. Correspondingly, the active intermediate enolic species predominate during the ethanol-SCR. With the aid of  $^1\text{H}$  solid NMR, we found that after silver loading, the remaining hydroxyl groups on  $\text{Ag}/\text{Al}_2\text{O}_3$  decrease as follows: water-free ball milling  $>$  semiwet method  $>$  wet impregnation. This indicates that the presence of water strengthens the proton exchange from hydroxyl groups on the surface of alumina by silver species. Thus the mechanism for silver species anchored on the surface of alumina to form  $\text{Ag-O-Al}$  entities is partly unraveled.

#### AUTHOR INFORMATION

##### Corresponding Author

\*Tel: +86-592-6190990. E-mail: [hhe@iue.ac.cn](mailto:hhe@iue.ac.cn).

##### Notes

The authors declare no competing financial interest.

#### ACKNOWLEDGMENTS

The work was supported by the National Natural Science Foundation of China (21373261 and 21177142), Strategic Priority Research Program of the Chinese Academy of Sciences (XDB05050504) and the National High Technology Research and Development Program of China (863 Program, 2013AA065301).

#### REFERENCES

- (1) Burch, R.; Breen, J. P.; Meunier, F. C. A Review of the Selective Reduction of  $\text{NO}_x$  with Hydrocarbons under Lean-Burn Conditions with Non-Zeolitic Oxide and Platinum Group Metal Catalysts. *Appl. Catal., B* **2002**, *39*, 283–303.
- (2) Shimizu, K.; Satsuma, A. Selective Catalytic Reduction of  $\text{NO}$  over Supported Silver Catalysts—Practical and Mechanistic Aspects. *Phys. Chem. Chem. Phys.* **2006**, *8*, 2677–95.
- (3) Liu, Z.; Ihl Woo, S. Recent Advances in Catalytic Denoxification and Technology. *Catal. Rev.: Sci. Eng.* **2006**, *48*, 43–89.
- (4) Granger, P.; Parvulescu, V. I. Catalytic  $\text{NO}_x$  Abatement Systems for Mobile Sources: From Three-Way to Lean Burn after-Treatment Technologies. *Chem. Rev.* **2011**, *111*, 3155–207.
- (5) Liu, F. D.; Yu, Y. B.; He, H. Environmentally-Benign Catalysts for the Selective Catalytic Reduction of  $\text{NO}_x$  from Diesel Engines: Structure-Activity Relationship and Reaction Mechanism Aspects. *Chem. Commun.* **2014**, *50*, 8445–8463.
- (6) Iwamoto, M.; Yahiro, H.; Shin, H. K.; Watanabe, M.; Guo, J. W.; Konno, M.; Chikahisa, T.; Murayama, T. Performance and Durability of Pt-MFI Zeolite Catalyst for Selective Reduction of Nitrogen Monoxide in Actual Diesel-Engine Exhaust. *Appl. Catal., B* **1994**, *5*, L1–L6.
- (7) Konig, A.; Held, W.; Richter, T. Lean-Burn Catalysts from the Perspective of a Car Manufacturer. Early Work at Volkswagen Research. *Top. Catal.* **2004**, *28*, 99–103.
- (8) Kristiansen, T.; Mathisen, K. On the Promoting Effect of Water During  $\text{NO}_x$  Removal over Single-Site Copper in Hydrophobic Silica  $\text{Apd-Aerogels}$ . *J. Phys. Chem. C* **2014**, *118*, 2439–2453.
- (9) Hu, Y. H.; Griffiths, K. Selective Catalytic Reduction of  $\text{NO}$  by Hydrocarbons on a Stepped Pt Surface: Influence of  $\text{SO}_2$  and  $\text{O}_2$ . *J. Phys. Chem. C* **2015**, *119*, 19789–19801.
- (10) Mannikko, M.; Wang, X.; Skoglundh, M.; Harelind, H. Silver/Alumina for Methanol-Assisted Lean  $\text{NO}_x$  Reduction on the Influence of Silver Species and Hydrogen Formation. *Appl. Catal., B* **2016**, *180*, 291–300.
- (11) Dong, H. Y.; Shuai, S.; Li, R. L.; Wang, H. X.; Shi, X. Y.; He, H. Study of  $\text{NO}_x$  Selective Catalytic Reduction by Ethanol over  $\text{Ag}/\text{Al}_2\text{O}_3$  Catalyst on a Hd Diesel Engine. *Chem. Eng. J.* **2008**, *135*, 195–201.
- (12) Strom, L.; Carlsson, P.-A.; Skoglundh, M.; Harelind, H. Hydrogen-Assisted SCR of  $\text{NO}_x$  over Alumina-Supported Silver and Indium Catalysts Using C-2-Hydrocarbons and Oxygenates. *Appl. Catal., B* **2016**, *181*, 403–412.
- (13) Kim, M. K.; Kim, P. S.; Kwon, H. J.; Nam, I. S.; Cho, B. K.; Oh, S. H. Simulation of OHC/SCR Process over  $\text{Ag}/\text{Al}_2\text{O}_3$  Catalyst for Removing  $\text{NO}_x$  from Diesel Engine. *Chem. Eng. J.* **2012**, *209*, 280–292.
- (14) D'Agostino, C.; Chansai, S.; Bush, I.; Gao, C.; Mantle, M. D.; Hardacre, C.; James, S. L.; Gladden, L. F. Assessing the Effect of Reducing Agents on the Selective Catalytic Reduction of  $\text{NO}_x$  over  $\text{Ag}/\text{Al}_2\text{O}_3$  Catalysts. *Catal. Sci. Technol.* **2016**, *6*, 1661–1666.
- (15) Wang, J.; He, H.; Xie, S.; Yu, Y. Novel  $\text{Ag-Pd}/\text{Al}_2\text{O}_3\text{-SiO}_2$  for Lean  $\text{NO}_x$  Reduction by  $\text{C}_3\text{H}_6$  with High Tolerance of  $\text{SO}_2$ . *Catal. Commun.* **2005**, *6*, 195–200.
- (16) Sitshebo, S.; Tsolakis, A.; Theinnoi, K.; Rodriguez-Fernandez, J.; Leung, P. Improving the Low Temperature  $\text{NO}_x$  Reduction Activity over a  $\text{Ag-Al}_2\text{O}_3$  Catalyst. *Chem. Eng. J.* **2010**, *158*, 402–410.
- (17) Kamolpoph, U.; Taylor, S. F. R.; Breen, J. P.; Burch, R.; Delgado, J. J.; Chansai, S.; Hardacre, C.; Hengrasme, S.; James, S. L. Low-Temperature Selective Catalytic Reduction (SCR) of  $\text{NO}_x$  with n-Octane Using Solvent-Free Mechanochemically Prepared  $\text{Ag}/\text{Al}_2\text{O}_3$  Catalysts. *ACS Catal.* **2011**, *1*, 1257–1262.
- (18) He, H.; Li, Y.; Zhang, X.; Yu, Y.; Zhang, C. Precipitable Silver Compound Catalysts for the Selective Catalytic Reduction of  $\text{NO}_x$  by Ethanol. *Appl. Catal., A* **2010**, *375*, 258–264.
- (19) Kim, M. K.; Kim, P. S.; Baik, J. H.; Nam, I.-S.; Cho, B. K.; Oh, S. H. Denox Performance of  $\text{Ag}/\text{Al}_2\text{O}_3$  Catalyst Using Simulated Diesel Fuel–Ethanol Mixture as Reductant. *Appl. Catal., B* **2011**, *105*, 1–14.
- (20) Korhonen, S. T.; Beale, A. M.; Newton, M. A.; Weckhuysen, B. M. New Insights into the Active Surface Species of Silver Alumina

Catalysts in the Selective Catalytic Reduction of No. *J. Phys. Chem. C* **2011**, *115*, 885–896.

(21) She, X.; Flytzanistephanopoulos, M. The Role of Agoal Species in Silver–Alumina Catalysts for the Selective Catalytic Reduction of Nox with Methane. *J. Catal.* **2006**, *237*, 79–93.

(22) Chansai, S.; Burch, R.; Hardacre, C.; Breen, J.; Meunier, F. The Use of Short Time-on-Stream in Situ Spectroscopic Transient Kinetic Isotope Techniques to Investigate the Mechanism of Hydrocarbon Selective Catalytic Reduction (HC-SCR) of Nox at Low Temperatures. *J. Catal.* **2011**, *281*, 98–105.

(23) Yan, Y.; Yu, Y. B.; He, H.; Zhao, J. J. Intimate Contact of Enolic Species with Silver Sites Benefits the SCR of NOx by Ethanol over Ag/Al<sub>2</sub>O<sub>3</sub>. *J. Catal.* **2012**, *293*, 13–26.

(24) Deng, H.; Yu, Y.; Liu, F.; Ma, J.; Zhang, Y.; He, H. Nature of Ag Species on Ag/Gamma-Al<sub>2</sub>O<sub>3</sub>: A Combined Experimental and Theoretical Study. *ACS Catal.* **2014**, *4*, 2776–2784.

(25) Deng, H.; Yu, Y.; He, H. Discerning the Role of Ag-O-Al Entities on Ag/Gamma-Al<sub>2</sub>O<sub>3</sub> Surface in Nox Selective Reduction by Ethanol. *J. Phys. Chem. C* **2015**, *119*, 3132–3142.

(26) Shimizu, K.; Shibata, J.; Yoshida, H.; Satsuma, A.; Hattori, T. Silver-Alumina Catalysts for Selective Reduction of NO by Higher Hydrocarbons: Structure of Active Sites and Reaction Mechanism. *Appl. Catal., B* **2001**, *30*, 151–162.

(27) Yu, Y. B.; Zhao, J. J.; Yan, Y.; Han, X.; He, H. A Cyclic Reaction Pathway Triggered by Ammonia for the Selective Catalytic Reduction of NOx by Ethanol over Ag/Al<sub>2</sub>O<sub>3</sub>. *Appl. Catal., B* **2013**, *136*, 103–111.

(28) Kannisto, H.; Ingelsten, H. H.; Skoglundh, M. Ag-Al<sub>2</sub>O<sub>3</sub> Catalysts for Lean Nox Reduction-Influence of Preparation Method and Reductant. *J. Mol. Catal. A: Chem.* **2009**, *302*, 86–96.

(29) Părvulescu, V. I.; Cojocaru, B.; Părvulescu, V.; Richards, R.; Li, Z.; Cadigan, C.; Granger, P.; Miquel, P.; Hardacre, C. Sol-Gel-Entrapped Nano Silver Catalysts-Correlation between Active Silver Species and Catalytic Behavior. *J. Catal.* **2010**, *272*, 92–100.

(30) Ravel, B.; Newville, M. Athena, Artemis, Hephaestus: Data Analysis for X-Ray Absorption Spectroscopy Using Ifeffit. *J. Synchrotron Radiat.* **2005**, *12*, 537–541.

(31) He, H.; Yu, Y. Selective Catalytic Reduction of Nox over Ag/Al<sub>2</sub>O<sub>3</sub> Catalyst: From Reaction Mechanism to Diesel Engine Test. *Catal. Today* **2005**, *100*, 37–47.

(32) Breen, J. P.; Burch, R.; Hardacre, C.; Hill, C. J. Structural Investigation of the Promotional Effect of Hydrogen During the Selective Catalytic Reduction of Nox with Hydrocarbons over Ag/Al<sub>2</sub>O<sub>3</sub> Catalysts. *J. Phys. Chem. B* **2005**, *109*, 4805–4807.

(33) Shimizu, K.; Sugino, K.; Kato, K.; Yokota, S.; Okumura, K.; Satsuma, A. Formation and Redispersion of Silver Clusters in Ag-MFI Zeolite as Investigated by Time-Resolved Qxafs and Uv-Vis. *J. Phys. Chem. C* **2007**, *111*, 1683–1688.

(34) Wu, Q.; He, H.; Yu, Y. B. In Situ Drifts Study of the Selective Reduction of NOx with Alcohols over Ag/Al<sub>2</sub>O<sub>3</sub> Catalyst: Role of Surface Enolic Species. *Appl. Catal., B* **2005**, *61*, 107–113.

(35) Yu, Y.; Song, X.; He, H. Remarkable Influence of Reductant Structure on the Activity of Alumina-Supported Silver Catalyst for the Selective Catalytic Reduction of NOx. *J. Catal.* **2010**, *271*, 343–350.

(36) Meunier, F. C.; Breen, J. P.; Zuzaniuk, V.; Olsson, M.; Ross, J. R. H. Mechanistic Aspects of the Selective Reduction of NO by Propene over Alumina and Silver-Alumina Catalysts. *J. Catal.* **1999**, *187*, 493–505.

(37) Wischert, R.; Laurent, P.; Coperet, C.; Delbecq, F.; Sautet, P. Gamma-Alumina: The Essential and Unexpected Role of Water for the Structure, Stability, and Reactivity of "Defect" Sites. *J. Am. Chem. Soc.* **2012**, *134*, 14430–14449.

(38) Decanio, E. C.; Edwards, J. C.; Bruno, J. W. Solid-State <sup>1</sup>H Mas NMR Characterization of Gamma-Alumina and Modified Gamma-Aluminas. *J. Catal.* **1994**, *148*, 76–83.

(39) Jacobsen, C. J. H.; Topsoe, N. Y.; Topsoe, H.; Kellberg, L.; Jakobsen, H. J. Quantitative <sup>1</sup>H Mas NMR-Studies of Structurally Different OH Surface Groups on Eta-Al<sub>2</sub>O<sub>3</sub> and Mol-/Eta-Al<sub>2</sub>O<sub>3</sub> Catalysts. *J. Catal.* **1995**, *154*, 65–68.